[2] Xenellis J, Papadimitriou N, Nikolopoulos T, Maragoudakis P, Segas J, Tzagaroulakis A, et al. Intratympanic steroid treatment in idiopathic sudden sensorineural hearing loss: a control study. Otolaryngol Head Neck Surg 2006;134:940–5.
[3] Sahni RS, Paparella MM, Schachern PA, Goycoolea MV, Le CT. Thickness of the human round window membrane in different forms of otitis media. Arch Otolaryngol Head Neck Surg 1987;113:630–4.
[4] Alzamil KS, Linthicum Jr FH. Extraneous round window membranes and plugs: possible effect on intratympanic therapy. Ann Otol Rhinol Laryngol 2000;109:30–2.
[5] Crane BT, Minor LB, Della Santina CC, Carey JP. Middle ear exploration in patients with Meniere's disease who have failed outpatient intratympanic gentamicin therapy. Otol Neurotol 2009;30:619–24.
[6] Plontke SK, Zimmermann R, Zenner HP, Lowenheim H. Technical note on microcatheter implantation for local inner ear drug delivery: surgical technique and safety aspects. Otol Neurotol 2006;27:912–7.
[7] Plontke SK, Plinkert PK, Plinkert B, Koitschev A, Zenner HP, Lowenheim H, et al. Transtympanic endoscopy for drug delivery to the inner ear using a new microendoscope. Adv Otorhinolaryngol 2002;59:149–155.

Neurochem Res (2011) 36:1261–1269
DOI 10.1007/s11064-011-0416-3

ORIGINAL PAPER

Expression and Function of Sox21 During Mouse Cochlea Development

Makoto Hosoya · Masato Fujioka · Satoru Matsuda · Hiroyuki Ohba · Shinsuke Shibata · Fumiko Nakagawa · Takahisa Watabe · Ken-ichiro Wakabayashi · Yumiko Saga · Kaoru Ogawa · Hirotaka James Okano · Hideyuki Okano

Accepted: 21 January 2011 / Published online: 3 February 2011

Abstract The development of the inner ear is an orchestrated process of morphogenesis with spatiotemporally controlled generations of individual cell types. Recent studies have revealed that the Sox gene family, a family of evolutionarily conserved HMG-type transcriptional factors, is differentially expressed in each cell type of the mammalian inner ear and plays critical roles in cell-fate determination during development. In this study, we examined the expression pattern of Sox21 in the developing and adult murine cochlea. Sox21 was expressed throughout the sensory epithelium in the early otocyst stage but became restricted to supporting cells during adulthood. Interestingly, the expression in adults was restricted to the inner phalangeal, inner border, and Deiters' cells: all of these cells are in direct contact with hair cells. Evaluations of the auditory brainstem-response revealed that Sox21$^{-/-}$ mice suffered mild hearing impairments, with an increase in hair cells that miss their appropriate planar cell polarity. Taken together with the previously reported critical roles of SoxB1 families in the morphogenesis of inner ear sensory and neuronal cells, our results suggest that Sox21, a counteracting partner of the SoxB1 family, controls fine-tuned cell fate decisions. Also, the characteristic expression pattern may be useful for labelling a particular subset of supporting cells.

Keywords Inner ear · Cochlea · Development · Sox21 · Hair cell · Supporting cell

Special Issue: In Honor of Dr. Mikoshiba.

Electronic supplementary material The online version of this article (doi:10.1007/s11064-011-0416-3) contains supplementary material, which is available to authorized users.

M. Hosoya · M. Fujioka · S. Matsuda · H. Ohba · S. Shibata · F. Nakagawa · H. J. Okano · H. Okano (✉)
Department of Physiology, School of Medicine, Keio University, Tokyo, Japan
e-mail: hidokano@sc.itc.keio.ac.jp

M. Fujioka · T. Watabe · K. Wakabayashi · K. Ogawa
Department of Otolaryngology, Head and Neck Surgery, School of Medicine, Keio University, Tokyo, Japan

Y. Saga
Division of Mammalian Development and Mammalian Genetics, National Institute of Genetics, Mishima, Shizuoka, Japan

Introduction

The development of the inner ear requires a complex process of cellular morphogenesis. The first step is the specification of the otic placode in a region of ectoderm located adjacent to rhombomere 5, followed by its invagination to form the otocyst. Second, a subset of epithelial cells within the otocyst undergoes specification and develops into a sensory patch, whereas another subset delaminates and migrates to the medial and forms the cochleovestibular ganglion. Next, individual cells within the sensory patch start to differentiate into hair cells or supporting cells. This series of processes is controlled tightly and delicately by multiple molecular pathways in both a cell-intrinsic and a non-cell autonomous manner. Recently, an evolutionarily conserved transcriptional factor, Sox2, has been identified as one of the earliest markers of developing inner ear prosensory domains and had been shown to be a key player of multiple roles in cell-fate determination processes [1]. Sox2 is indeed an early permissive factor in the prosensory domain formation required for hair cell formation [1] and neuronal formation in the developing mammalian inner ear [2].

There are five Sox proteins that have been categorized as Group B Sox, which share evolutionarily conserved DNA binding domains (HMG domains) plus SoxB consensus. In contrast to the Group B1 Sox (Sox1, 2 and 3), which contain a typical activator domain at their C-terminal, Sox 14 and Sox21 are classified as Group B2 because they contain a functional repressor domain [3, 4]. Consistent with these structural biochemical characteristics, Sox1/2/3 were reported to suppress neuronal differentiation by maintaining the undifferentiated state of neural precursor cells during developmental [5–10], while Sox21 promotes neurogenesis in chicken embryonic spinal cord by counteracting Sox1/2/3 [11]. In the inner ear, the expression of Sox21 in the developing chicken has been reported, but the precise time-dependent changes that occur during development remain unknown. Here, we examined the expression profile of Sox21 at several time points using knock-in mice harboring EGFP at the Sox21 locus [12]. We found that Sox21 was expressed throughout the sensory epithelium in developing cochlea in mice. During the process of morphogenesis, Sox21 showed a unique expression pattern, and its expression was restricted in supporting cells that were in direct contact with hair cells: the inner phalangeal cells, the inner border cells, and Deiters' cells in adults. Regarding hearing functions, $Sox21^{-/-}$ mice exhibited a mild hearing impairment according to an auditory brainstem-response (ABR) analysis, together with an increase in hair cells that had lost their appropriate planar cell polarity.

Experimental Procedures

Animal

All animal care and treatment procedures were performed in accordance with institutional guidelines approved by the Experimental Animal Care Committee of the Keio University School of Medicine. Animals were housed in a room with a 12-h light/dark cycle and were fed ad libitum. *Sox21*$^{-/-}$mice were established as described previously [12] and were maintained on a C57Bl6/J background.

Immunohistochemistry

Animals were perfused with 4% paraformaldehyde (PFA; Nakalai Tesque), and the temporal bones were dissected, fixed in 4% PFA at 4°C overnight, decalcified with Decalcifying Solution. B (Wako) for 48–72 h if needed, and sliced into 6 μm sections then embedded in Tissue-Tek O.C.T. compound. The sections were preblocked for 1 h at room temperature in 10% normal serum in PBS or in 0.1% TritonX-100 (Sigma) in 10% normal serum in PBS (for anti—Myo7a and anti—NeuroD antibodies), incubated with primary antibodies at 4°C overnight, and incubated with Alexa Fluor-conjugated secondary antibodies for 60 min at room temperature. The nuclei were counterstained with Hoechst 33342. Following is the number of $Sox21^{+/EGFP}$ mice used at each stage: E10.5; $n = 3$, E16.5; $n = 3$, P0; $n = 3$, P9; $n = 3$, P14; $n = 2$, Adult; $n = 4$.

Antibodies

The primary antibodies used in this study were as follows: anti-Sox2 (goat IgG, Santa Cruz Biotechnology sc-17320, 1:100), anti-Sox21 (goat IgG, R&D AF3538, 1:100), anti-Myo7a (rabbit IgG, PROTEUS BioScience 25-6790, 1:250), anti-GFP (rabbit IgG, Medical & Biological Laboratory [MBL] 598, 1:500; goat IgG, ROCKLAND 600-101-215, 1:200), anti-NeuroD (goat IgG, santa Cruz Biotechnology sc1084, 1:100). Immunoreactivity was visualized using Alexa Fluor-conjugated secondary antibodies (Molecular Probes, 1:500). F-Actin was stained using rhodamine-phalloidin (Invitrogen R415, 1:40).

RT-PCR

The otic vesicle from E10.5 and the organ of Corti and the spiral ganglion plus Kölliker's organ from E15, P1 and P9 were dissected from wild-type C57BL/6Jcl mice under a microscope. mRNA and cDNA were prepared using an RNeasy mini kit (Qiagen) and SuperScript II (Invitrogen) according to the manufacturer's protocol. The primers for Sox21 and GAPDH were as follows, respectably: Sox21f, 5′-CACACACGTGTACATATGTA-3′; Sox21r, 5′-TCA AAACGCAACAGGTTCCG-3′; GAPDHfwd, 5′-AACGG GAAGCCCATCACC-3′; GAPDHrev, 5′-CAGCCTTGGC AGCACCAG-3′.

Whole Mount Embryo

Whole embryos of $Sox21^{+/EGFP}$ mice at E10.5 were fixed in 4% PFA and observed under a fluorescent microscope. Genotyping was confirmed retrospectively from the tail tips of each embryo as described previously [12].

Surface Preparation and Scanning Electron Microscopy (SEM)

The detailed histology of the adult organ of Corti was examined using flat-mounted surface preparations using previously reported materials and methods [13]. The prepared specimens were stained with F-actin and/or EGFP in $Sox21^{EGFP/EGFP}$, $Sox21^{+/EGFP}$ and wild-type mice ($n = 7$, 4 and 2, respectively). The ultrastructure of their surfaces

was examined using SEM in Sox21$^{EGFP/EGFP}$, Sox21$^{+/EGFP}$ and wild-type mice ($n = 2$, 3, and 3, respectively) according to a previously reported protocol [14].

Auditory Brainstem Response (ABR)

To test the auditory function of Sox21 knock-out mice, the ABR was measured in Sox21$^{EGFP/EGFP}$ and litter mate wild-type mice ($n = 4$ and 3, respectively) according to previously reported methods [15].

Results

We first performed RT-PCR for *Sox21* in the developing inner ear (Fig. 1A). *Sox21* was detected at E10.5 in the otic vesicle. At E15 and P1, *Sox21* was detected in both the organ of Corti and the Kölliker's organ. At P9, the expression in the Kölliker's organ had decreased, and no expression was detected. In contrast, the expression in the organ of Corti was maintained.

We then further analyzed the expression pattern of EGFP in Sox21$^{+/EGFP}$ mice. To confirm that the EGFP expression in the Sox21$^{+/EGFP}$ knock-in mice recapitulates the endogenous Sox21 protein expression, we double-stained for EGFP and Sox21 on cochlear cross sections of Sox21$^{+/EGFP}$ mice using anti–Sox21 and anti–GFP antibody (Supplementary Fig. S1). As shown in Fig. S1, all of the nuclei in the EGFP-positive cells were labeled with anti-Sox21 antibody, while none of the nuclei in the EGFP-negative cells were labeled. This result indicates that the EGFP expression pattern in Sox21$^{+/EGFP}$ mice reflects the endogenous protein expression of Sox21. In mouse embryos at E10.5, strong fluorescence for Sox21/EGFP was observed widely in the CNS stem cell areas. Also, EGFP was observed in the otocyst (Fig. 1B). Detailed expression in the coronal sections of the E10.5 otocyst showed that the Sox21/EGFP immunoreactivity was stronger on the ventral-lateral side, while that of Sox2 was stronger on the ventral and weaker on the dorsal side (Fig. 1C, D). The expressions of Sox2 and Sox21/EGFP were overlapped strongly on the ventral side of the otocyst, where the future cochlea was formed. In the ventral to medial region of the otic vesicle, Sox2-immunoreactivity was predominant, while Sox21/EGFP-immunoreactivity was predominant on the ventral to lateral side. At this stage, delaminated neurons from the epithelium start to form the spiral ganglion. Immunostaining showed that both EGFP and Sox2 expressions were observed in the developing spiral ganglion cells and were co-labeled with NeuroD, an early stage neuronal marker [16] (Fig. 1D-1, 2 and E-2, 3 arrows). Note that the EGFP-expression levels in the neurons were weaker than those in the future sensory epithelium region.

Cells in the organ of Corti differentiate into hair cells and supporting cells at E16.5. At E17, Sox2-expression is limited to a domain that includes both the prosensory and adjacent areas of the LER and GER [17–19]. At this stage, EGFP-immunoreactivity was widely observed in half of the cochlear duct from the apex to the base (Fig. 2A–C). Most of the Sox2-positive area was covered by a Sox21/EGFP-positive domain, both in the hair cell layer and the supporting cell layer of the sensory epithelium and GER, except in the Hensen's cells which are located in the most lateral rows of the future sensory epithelium and were positive for Sox2. Interestingly, no expression was detected in the spiral ganglion (Fig. 2A-3, B-3, arrow).

The structure of the tunnel of Corti is formed during the first two postnatal weeks in mice. At P0, Sox2-expression has been reported in a subset of differentiated supporting cells including Deiters', pillar, inner phalangeal and Hensen's cells [1]. The Sox21/EGFP-immunoreactivity was observed in Deiters' cells, pillar cells and inner phalangeal cells and Kölliker's organ (Fig. 2D, E), and the immunoreactivity in hair cells, which had been observed up to E16.5, had disappeared. No EGFP expression was observed in Sox2-positive Hensen's cells (Fig. 2E-1, arrowhead).

At P9, the tunnel of Corti had not yet been formed completely, but the developing pillar cells clearly showed their structure. At this stage, the EGFP-immunoreactivity was observed only in supporting cells, including Deiters', pillar, inner phalangeal, inner border and Hensen's cells, but the immunoreactivity in Kölliker's organ had disappeared (Fig. 3A–C). The levels of EGFP-immunoreactivity in the medial two rows of Deiters' cells, inner border cells and inner phalangeal cells were stronger, compared with the most lateral row of Deiters' cells and pillar cells. Note that the expression of Sox21/EGFP in the Sox2-positive Hensen's cells, which had not been observed at P0, had clearly re-emerged at this stage (Fig. 3B-1 arrow). Interestingly, some cells in the auditory nerve were positive for Sox21/EGFP. These cells are likely oligodendrocytes or astrocytes because the nerve fibers in the auditory nerve are axons originating from spiral ganglion neurons, of which the somas were negative for EGFP (Fig. 3A-2 arrowhead).

At P14, the structure of the organ of Corti had been almost completely formed. The Sox21/EGFP-immunoreactivity was observed in three rows of Deiters' cells, inner phalangeal cells, inner border cells and a part of Hensen's cells at this stage (Fig. 3D). The expression in the pillar cells, which were observed at P9, had disappeared, while the expression in the most lateral row of Deiters' cells was observed. The gradient of immunoreactivity for Sox21/EGFP in the Deiters' cells, which was observed at P9, was not detected at this stage.

In adults, the Sox21/EGFP-immunoreactivity was observed only in the Deiters' cells, the inner border cells,

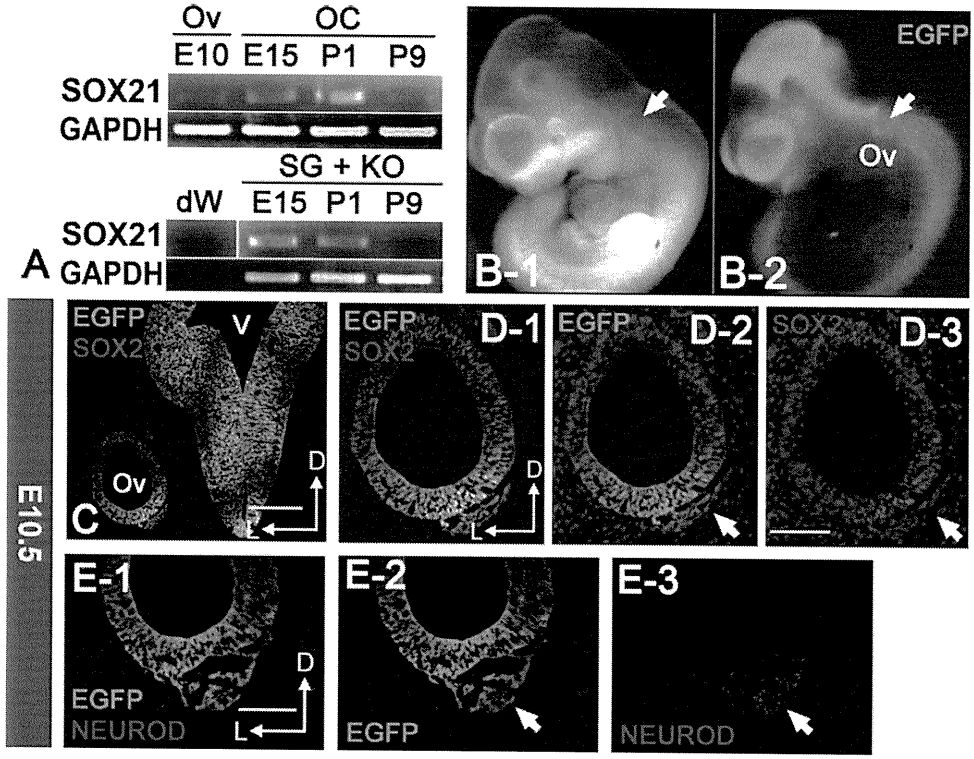

Fig. 1 Expression of Sox21 in developing inner ear. **A** RT-PCR analysis of Sox21 in wild-type mice. Sox21 was expressed in the otic vesicle at E10.5 and was detected in both the organ of Corti and the Kölliker's organ at E15 and P1, while at P9, the expression persisted only in the organ of Corti and had diminished in the spiral limbs to an undetectable level. *Ov* Otic vesicle, *OC* organ of Corti, *SG* spiral ganglion, *KO* Kölliker's organ. **B** Expression of Sox21/EGFP in E10.5 $Sox21^{+/EGFP}$ knock-in mice. At E10.5, strong EGFP-immunoreactivity was broadly observed in the CNS stem cell areas as well as the otocyst (**B-1**, **B-2** *arrows*). **C**, **D**, **E** Sox21/EGFP-expression in E10.5 inner ear. Sox21/EGFP (*green*) co-labeled with Sox2 (*red*, in **C** and **D**) and NeuroD (*red*, in **E**) in E10.5 mouse developing inner ear. In **D-2**, **3** the nuclei were counterstained with Hoechst (*blue*). Within the sensory epithelium, stronger Sox21/EGFP-expression was observed on the ventral lateral side, while for Sox2-expression, the expression was stronger on the ventral plus dorsal side. Both Sox21/EGFP and Sox2 expressions were observed in the delaminating spiral ganglion neurons (**D-2**, **D-3** *arrow*), that were colabeled with NeuroD (**E-2**, **3** *arrow*). (**C** *OV* otic vesicle, *V* fourth ventricle, Scale bar: 200 μm in **C**, 100 μm in **D**, 100 μm in **E**)

and the inner phalangeal cells. In all the rows of Deiters' cells, Sox21/EGFP-immunoreactivity was observed (Fig. 4A, B). The immunoreactivity in Hensen's cells, which were observed at P9 and P14, had disappeared.

We have already confirmed that the expression of Sox21 protein was completely abolished in homozygotes (i.e., $Sox21^{EGFP/EGFP}$) [12]. Histological analyses using a scanning electron microscope (SEM) showed that two of nine homozygote mice exhibited an increase in hair cells (Fig. 5). Interestingly, the polarity of the extra hair cells in the affected mice was disorganized, while rest of the hair cells in the same animal were normal (Fig. 5a–c). Finally, the hearing function of Sox21 knock-out mice was measured using ABR (Fig. 5d). The ABR threshold was slightly but significantly higher in the knock-out mice, compared with that in the wild-type mice, at both 8 and 16 kHz ($P < 0.05$). Thresholds of individual mice are documented in Supplementary Fig. S2.

Discussion

We showed that Sox21 was expressed in cochlear sensory epithelium throughout development but was progressively restricted to supporting cells in the mature organ of Corti: Sox21 was expressed in a broad domain containing the entirety of the future sensory epithelium at E10.5, and the expression was restricted to the inner phalangeal cells and the Deiters' cells as the inner ear matured. During this process, Sox21 showed distinctive expression patterns, as revealed by EGFP-immunoreactivity: temporally at P9, the expression level of Sox21 was not equal but exhibited a

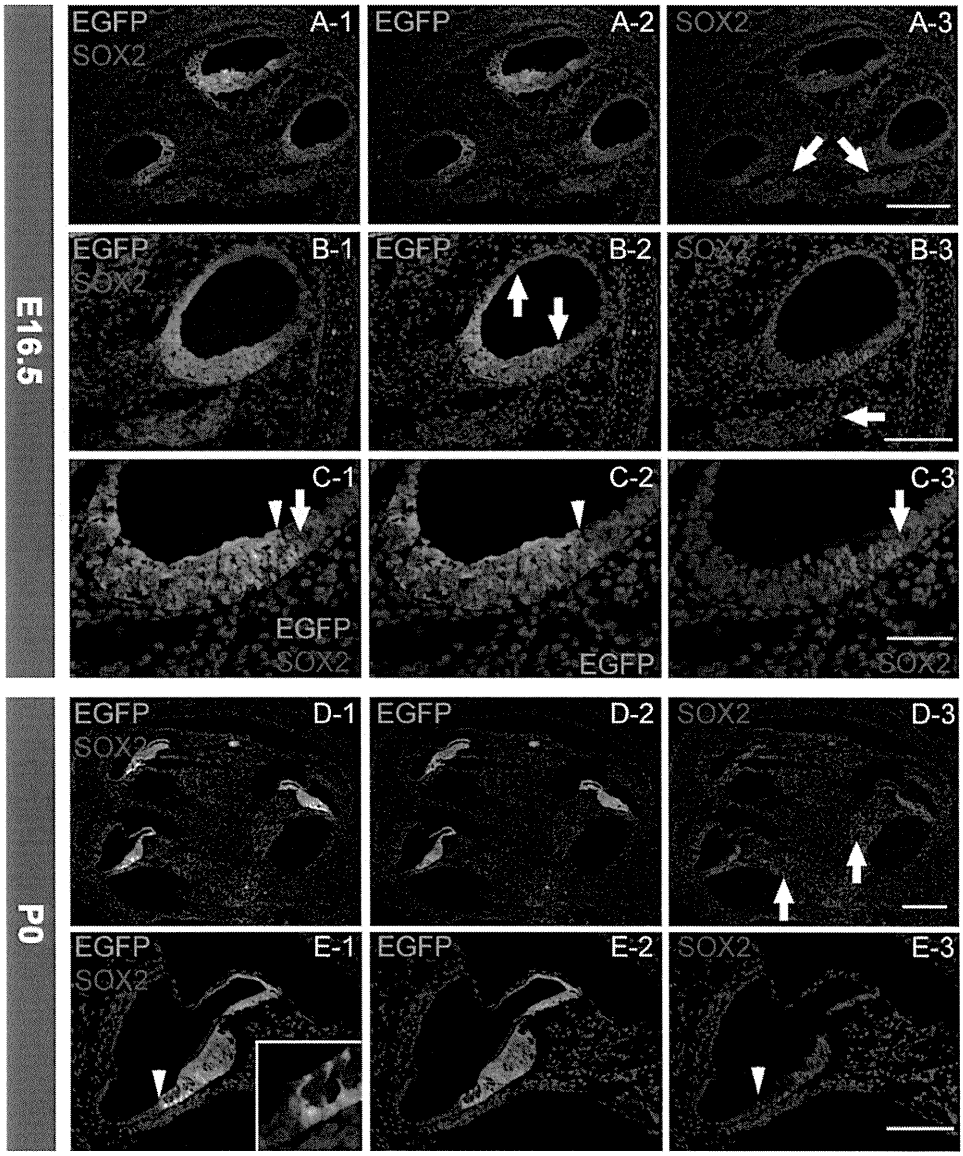

Fig. 2 Sox21/EGFP expression in the developing inner ear. **A C** Sox21/EGFP expression in E 16.5 mouse embryos. Sox21/EGFP (*green* **A-1**, **A-2**, **B-1**, **B-2**, **C-1**, and **C-2**) and Sox2 (*red* **A-1**, **A-3**, **B-1**, **B-3**, **C-1**, and **C-3**) expression patterns in E16.5 mouse developing inner ear. In each image, the nuclei were counterstained with Hoechst (*blue*). Sox21/EGFP-expression was observed only within the modiolar half of the cochlear duct (**B-2** between *arrows*), but no expression was observed in the spiral ganglion, while Sox2 expression was observed both in the future sensory epithelium and the spiral ganglion (**A-3**, **B-3** *arrow*). Note that, in the cochlea duct, the Sox21/EGFP-expression domain was wider than the region of sensory epithelium marked by Sox2 except in the Sox2-positive Hensen's cells (**C-1**, **2**, **3**; *arrow*, *arrowhead*). (Scale bar: 200 μm in **A**, 100 μm in **B**, 50 μm in **C**). **D E** Sox21/EGFP-expression in the neonate mice. Sox21/EGFP (*green* **D-1**, **D-2**, **E-1** and **E-2**) and Sox2 (*red* **D-1**, **D-2**, **E-1** and **E-3**). In each image, the nuclei were counterstained with Hoechst (*blue*). By birth, the EGFP immunoreactivity had disappeared from the hair cells, but persisted in the supporting cells except the Sox2-positive Hensen's cells (**E-1** *arrow head*). Sox21/EGFP-expression was not observed in the spiral ganglion, where Sox2 was observed. (**D-3** *arrow*) (Scale bar: 200 μm in **D**, 100 μm in **E**)

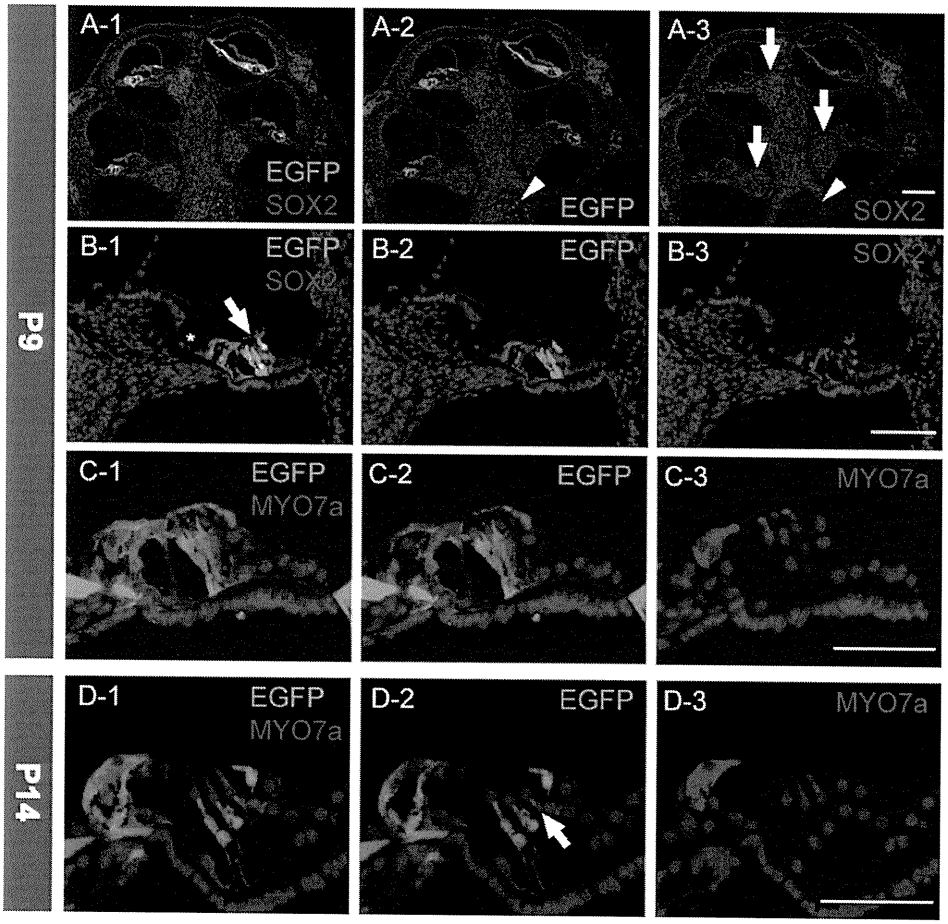

Fig. 3 Expression of Sox21/EGFP in the postnatal cochlea. **A C** Sox21/EGFP-expression at P9. Sox21/EGFP (*green* **A-1**, **A-2**, **B-1**, **B-2**, **C-1** and **C-2**), Sox2 (*red* **A-1**, **A-3**, **B-1** and **B-3**) and Myosin 7a (*red* **C-1** and **C-3**). In each image, the nuclei were counterstained with Hoechst (*blue*). Sox21/EGFP expression was not observed in the spiral ganglion, while Sox2 expression was consistently observed (**A-3** *arrow*). EGFP-expression was observed in the inner phalangeal cells, medial two rows of Deiters' cells, inner border cells, pillar cells and Sox2-positive Hensen's cell (**B-1** *arrow*). Some cells in the central portion of auditory nerve were positive for both Sox21/EGFP and Sox2, most likely oligodendrocytes or astrocytes. (**A-2** and **A-3** *arrowhead*) (**B**) Sox21/EGFP expression was not observed in hair cells (**C**) and the GER or spiral limbs (**B-1** *asterisk*). The expression of Sox21/EGFP in Deiters' cells, inner border cells and inner phalangeal cells was strong, but was relatively weak in the most lateral row of Deiters' cells and the pillar cells. (**B-2**, **C-2**) (Scale bar: 200 μm in **A**, 100 μm in **B**, 50 μm in **C**). **D** Sox21/EGFP expression in P14 organ of Corti. Sox21/EGFP (*green* **D-1** and **D-2**) and Myosin 7a (*red* **D-1** and **D-3**). In each image, the nuclei were counterstained with Hoechst (*blue*). EGFP-expression was observed only in the inner phalangeal cells, inner border cells, three rows of Deiters' cells and part of Hensen's cell. **D** EGFP expression was observed in the most lateral row of Deiters' cells. No apparent gradient of expression was observed among the Deiters' cells (**D-2** *arrow*). In the pillar cells, EGFP expression was diminished and no longer observed, while it was observed at P9. (Scale bar: 50 μm in **D**)

gradient among the three rows of the Deiters' cells, with high expression in the modiolar two rows and low expression in the lateral row (Fig. 4C). The expression once again became homogenous at P14. This phenomenon was accompanied by the temporal expression of EGFP in the Hensen's cells between P9 and P14, which did not become positive until P0 and after P28. These findings may indicate that the three rows of Deiters' cells are not the same with respect to their characteristics as potential progenitor cells, at least during the development process, leading us to speculate that Sox21 might be involved in the delicate spatiotemporal maturation of individual supporting cells.

The physiological function of Sox21 appears to depend on the cellular context in a neuronal cell line [11, 20].

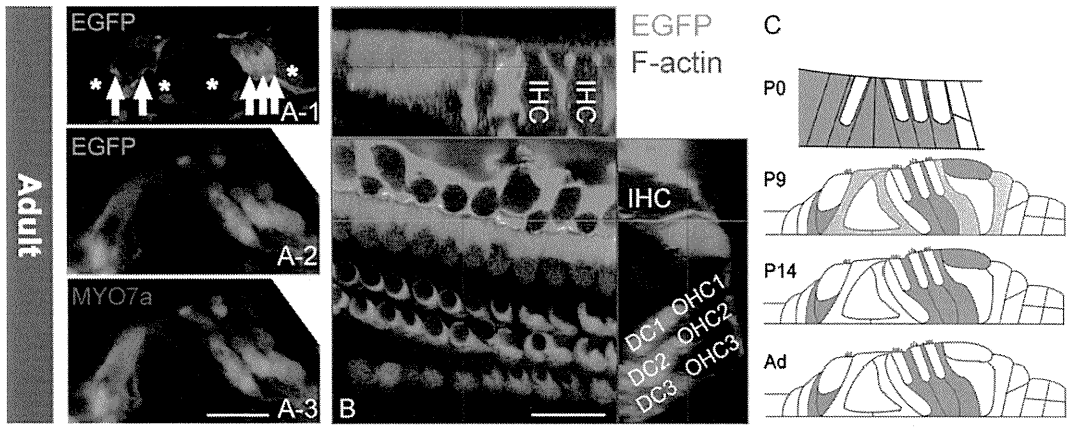

Fig. 4 Sox21/EGFP expression in adult. **A B** Sox21/EGFP expression in adult organ of Corti. Sox21/EGFP (*green* **A-1**, **A-2**, **A-3** and **B**), Myosin 7a (*red* **A-3**) and F-actin (*red* **B**). The nuclei were counterstained with Hoechst (*blue*). In the adult (4 weeks old) cochlea, EGFP-immunoreactivity was observed only in supporting cells that directly contacted with the hair cells: Deiter' s cell, inner border cells and inner phalangeal (**A-1** *arrows*). Note that no expression was observed in hair cells, pillar cells, Hensen's cells (**A-1** *asterisks*). (Scale bar: 25 μm in **A**, 25 μm in **B**). **C** Schema of Sox21/EGFP-expression pattern in the developing cochlea. Summary of the distinctive expression patterns of Sox21 in the developing organ of Corti. At P0, EGFP expression was observed in supporting cells except Sox2-positive Hensen's cells and the modiolar half of the cochlear duct. No immunoreactivity was observed in the hair cells. At P9, EGFP expression was observed only in supporting cells. The immunoreactivity observed in the inner phalangeal cells, inner border cells, medial two rows of Deiters' cells, and part of the Hensen's cells was strong, while the immunoreactivity observed in the most lateral Deiters' cells and pillar cells was relatively weak. At P14, the expression was observed in inner phalangeal cells, inner border cells, three rows of Deiters' cells, and part of the Hensen's cells. In adults, the expression was observed only in the inner phalangeal cells, inner border cells, and Deiters' cells (Ad: Adult)

Notably, in the skin, we found that Sox21 is required for the fine-tuned differentiation of hair shafts and is required for the formation of the cuticle, which is essential for the solid junction of hairs and follicles of the skin [12]. During the development of the inner ear, previous reports have revealed that Sox2 is required for the prosensory domain formation of the cochlea: mouse mutants with no or reduced expression of Sox2 in the developing inner ear develop a severe inner ear malformation with no or a reduced number of hair cells [17]. Previous reports have revealed that Sox21 is the only Group B2 Sox expressed in the cochlea throughout development [3, 4]. Here, we found that the distinctive spatiotemporal changes of Sox21 expression in the developing cochlea partially overlapped with those of the Group B1 Sox family, including Sox2. Although the role of Sox21 in the developing and adult inner ear remains to be elucidated, Sox21 may counteract Sox2 in developing prosensory cells to control the fine-tuned formation of hair cells. In addition, Sox21 might also be responsible for the differentiation of particular subsets of supporting cells, such as Deiter's and phalangeal cells, as is also the case with hair shaft differentiation in the skin. Further analyses of Sox21 mutant mice should help to solve this question.

At E10.5, Sox21 was expressed in the developing spiral ganglion, but no expression was observed after E16, in contrast to the expression of Sox2 observed throughout the process of developing cochleovestibular neurons, as previously reported [19]. In addition, Sox2 was also known to induce neuronal formation in the developing mammalian cochlea [2]. Our findings suggest that, unlike developing spinal cord [11], the differentiation of the cochleovestibular ganglion might not be dependent on Sox21.

The phenotypes of homozygote Sox21 knock-in and knock-out mice seem intriguing. The increase in hair cells was severer for the outer hair cells and lesser for the inner hair cells, similar to observations in Hes5 knock-out mice [21]. Although the penetrance of the phenotype was approximately 20%, the data suggests that sensory epithelium formation might possibly be mediated by Notch-related genes, such as Hes5. Further study to understand the role of Sox21 in both hair cells and subsets of supporting cells should be attempted, particularly the downstream target genes of Sox21.

Previous studies have shown that supernumerous hair cells lead to severe hearing loss; for instance, in pRb conditional knock-out mice, the hearing threshold was severely affected by 40 dB as a result of the delayed cell death, while each hair cell had a functional mechano-transduction channel [22]. In contrast, in Sox21 knock-out mice, the hearing impairment was as slight as 10 dB; an increase in hair cells was observed, but the increase was

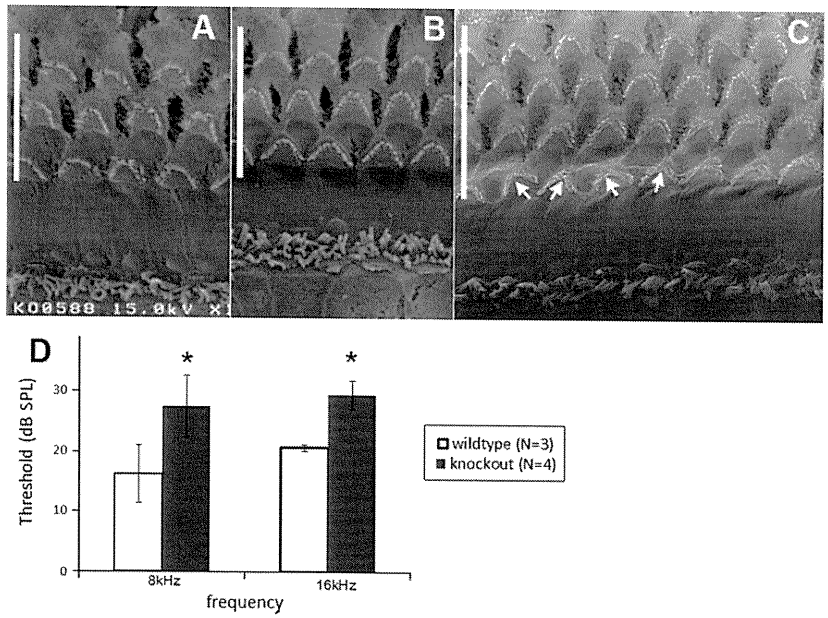

Fig. 5 Phenotype of Sox21$^{EGFP/EGFP}$ or Sox21 knock-out mice in adults. **a** c Extra hair cells in Sox21 $^{-/-}$ missing planar cellular polarity. Scanned electron microscopy images of wild-type, Sox21$^{+/-}$ and Sox21 $^{-/-}$ mice (**a**, **b** and **c**, respectively). In the knock-out mice, supernumerary outer hair cells (*OHCs*) were observed from the basal to apical turns. The first row of OHCs missed their polarities (*arrows*), while the others seemed normal (**c**). **d** Slight but significant impairment of hearing in Sox21 knock-out mice. An auditory brainstem response (*ABR*) analysis was performed in Sox21 $^{-/-}$ mice and litter mate wild-type mice ($n = 4$ and 3, respectively) at 8 and 16 kHz. The hearing threshold was significantly elevated in the knock-out mice, compared with the wild-type mice, but only by 10 dB at both frequencies ($^*P < 0.05$, Mann Whitney U test)

not as severe as that in the pRB conditional knock-out mice and the structure of the organ of Corti—one layer of hair cells lying over a layer of supporting cells—was completely preserved. Our findings do not lead to the conclusion that the hearing impairment was due to the increase in hair cells because Sox21 expression was observed not only in the supporting cells, but also in the auditory nerve, most likely in oligodendrocytes or astrocytes. However, these results suggest that not only a sufficient number, but also an appropriate physiological structure for the hair cells is required for the function of the organ of Corti. Regaining a suitable number of hair cells at the correct position or on the supporting cells may be important for a functional outcome in regenerative medicine for patients with hearing loss.

Unlike some supporting cell markers including GFAP [23], S100A1 [24], Prox1 [25], TC2 [26], p75^{NTR} [27], Jagged1 [28], GLAST [29] and Sox2 [18, 19], Sox21 expression persists into adulthood, especially in Deiters' cells, inner border cells and phalangeal cells. Supporting cells in the organ of Corti include several distinct subpopulations that are morphologically different, yet only three types of cells are in direct contact with the hair cells: the inner phalangeal cells, the inner border cells, and Deiters' cells. Our results clearly demonstrated that Sox21 expression was observed only in the supporting cells that are in direct contact with the hair cells in adult cochlea. This finding shows that Sox21 is a novel marker of supporting cells neighboring hair cells. Moreover, the results suggest that genetic modification using the Sox21 locus, such as Cre knock-in, may be a useful tool for targeting supporting cells that are in direct contact with hair cells, including specific gene expression. Furthermore, gene delivery or therapy using a Sox21 enhancer or promoter may have feasible clinical applications, particularly for inducing hair cells at the proper positions, as discussed previously.

In conclusion, we showed that Sox21 is expressed in developing and adult cochlea. A broad expression of Sox21, including the otocyst and delaminating neurons, became restricted to supporting cells, and finally was only expressed in cells in direct contact with hair cells. Since the expression pattern was extremely distinctive, this pattern may be useful for labeling a subset of supporting cells in detailed analyses of the organ of Corti. Furthermore, our findings in Sox21 knock-out mice indicate that Sox21 plays

an important role in the development and in the physiological function of the cochlea. Further analyses examining the function of this intriguing repressor Sox B protein in supporting and hair cell differentiation are awaited in the near future.

Acknowledgments We thank Ms. Ayano Mitsui and Dr. T. Nagai for their technical assistance and Dr. Junko Murata (Osaka University) for technical advices. This work was supported by grants from the Ministry of Education, Culture, Sports, Science and Technology (MEXT), the Japan Science and Technology Corporation (JST), and the Funding Program for World-leading Innovative R&D on Science and Technology to H.O., and by a Grant-in-Aid for Scientific Research B (20390444) to K.O., and by a Research on Measures for Intractable Diseases from the Ministry of Health, Labor and Welfare of Japan to M.F., and by a Keio University grant-in-aid for encouragement of young medical scientists to M.F., and by a Keio Gijuku Academic Development Funds to M.F. and by a Grant-in-Aid for Young Scientists B (22791628) to M.F. from MEXT. and by a grant-in-aid from the Global COE Program of MEXT, Japan to Keio University.

References

1. Dabdoub A, Puligilla C, Jones JM et al (2008) Sox2 signaling in prosensory domain specification and subsequent hair cell differentiation in the developing cochlea. Proc Natl Acad Sci USA 105:18396–18401
2. Puligilla C, Dabdoub A, Brenowitz SD et al (2010) Sox2 induces neuronal formation in the developing mammalian cochlea. J Neurosci 30:714–722
3. Uchikawa M, Kamachi Y, Kondoh H (1999) Two distinct subgroups of Group B Sox genes for transcriptional activators and repressors: their expression during embryonic organogenesis of the chicken. Mech Dev 84:103–120
4. Bowles J, Schepers G, Koopman P (2000) Phylogeny of the SOX family of developmental transcription factors based on sequence and structural indicators. Dev Biol 227:239–255
5. Bani-Yaghoub M, Tremblay RG, Lei JX et al (2006) Role of Sox2 in the development of the mouse neocortex. Dev Biol 295:52–66
6. Bylund M, Andersson E, Novitch BG et al (2003) Vertebrate neurogenesis is counteracted by Sox1-3 activity. Nat Neurosci 6:1162–1168
7. Favaro R, Valotta M, Ferri AL et al (2009) Hippocampal development and neural stem cell maintenance require Sox2-dependent regulation of Shh. Nat Neurosci 12:1248–1256
8. Ferri AL, Cavallaro M, Braida D et al (2004) Sox2 deficiency causes neurodegeneration and impaired neurogenesis in the adult mouse brain. Development 131:3805–3819
9. Kan L, Israsena N, Zhang Z et al (2004) Sox1 acts through multiple independent pathways to promote neurogenesis. Dev Biol 269:580–594
10. Wang TW, Stromberg GP, Whitney JT et al (2006) Sox3 expression identifies neural progenitors in persistent neonatal and adult mouse forebrain germinative zones. J Comp Neurol 497: 88–100
11. Sandberg M, Kallstrom M, Muhr J (2005) Sox21 promotes the progression of vertebrate neurogenesis. Nat Neurosci 8:995–1001
12. Kiso M, Tanaka S, Saba R et al (2009) The disruption of Sox21-mediated hair shaft cuticle differentiation causes cyclic alopecia in mice. Proc Natl Acad Sci USA 106:9292–9297
13. Masuda M, Nagashima R, Kanzaki S et al (2006) Nuclear factor-kappa B nuclear translocation in the cochlea of mice following acoustic overstimulation. Brain Res 1068:237–247
14. Mizutari K, Fujioka M, Nakagawa S et al (2010) Balance dysfunction resulting from acute inner ear energy failure is caused primarily by vestibular hair cell damage. J Neurosci Res 88:1262–1272
15. Fujioka M, Kanzaki S, Okano HJ et al (2006) Proinflammatory cytokines expression in noise-induced damaged cochlea. J Neurosci Res 83:575–583
16. Lawoko-Kerali G, Rivolta MN, Lawlor P et al (2004) GATA3 and NeuroD distinguish auditory and vestibular neurons during development of the mammalian inner ear. Mech Dev 121: 287–299
17. Kiernan AE, Pelling AL, Leung KK et al (2005) Sox2 is required for sensory organ development in the mammalian inner ear. Nature 434:1031–1035
18. Hume CR, Bratt DL, Oesterle EC (2007) Expression of LHX3 and SOX2 during mouse inner ear development. Gene Expr Patterns 7:798–807
19. Mak AC, Szeto IY, Fritzsch B et al (2009) Differential and overlapping expression pattern of SOX2 and SOX9 in inner ear development. Gene Expr Patterns 9:444–453
20. Ohba H, Chiyoda T, Endo E et al (2004) Sox21 is a repressor of neuronal differentiation and is antagonized by YB-1. Neurosci Lett 358:157–160
21. Zine A, Aubert A, Qiu J et al (2001) Hes1 and Hes5 activities are required for the normal development of the hair cells in the mammalian inner ear. J Neurosci 21:4712–4720
22. Sage C, Huang M, Vollrath MA et al (2006) Essential role of retinoblastoma protein in mammalian hair cell development and hearing. Proc Natl Acad Sci USA 103:7345–7350
23. Rio C, Dikkes P, Liberman MC et al (2002) Glial fibrillary acidic protein expression and promoter activity in the inner ear of developing and adult mice. J Comp Neurol 442:156–162
24. Coppens AG, Kiss R, Heizmann CW et al (2001) Immunolocalization of the calcium binding S100A1, S100A5 and S100A6 proteins in the dog cochlea during postnatal development. Brain Res Dev Brain Res 126:191–199
25. Bermingham-McDonogh O, Oesterle EC, Stone JS et al (2006) Expression of Prox1 during mouse cochlear development. J Comp Neurol 496:172–186
26. Bianchi LM, Liu H, Krug EL et al (1999) Selective and transient expression of a native chondroitin sulfate epitope in Deiters' cells, pillar cells, and the developing tectorial membrane. Anat Rec 256:64–71
27. Sato T, Doi K, Taniguchi M et al (2006) Progressive hearing loss in mice carrying a mutation in the p75 gene. Brain Res 1091: 224–234
28. Murata J, Tokunaga A, Okano H et al (2006) Mapping of notch activation during cochlear development in mice: implications for determination of prosensory domain and cell fate diversification. J Comp Neurol 497:502–518
29. Jin ZH, Kikuchi T, Tanaka K et al (2003) Expression of glutamate transporter GLAST in the developing mouse cochlea. Tohoku J Exp Med 200:137–144

Eur Arch Otorhinolaryngol (2011) 268:973–978
DOI 10.1007/s00405-011-1484-3

OTOLOGY

Acoustic overstimulation-induced apoptosis in fibrocytes of the cochlear spiral limbus of mice

Yong Cui · Guang-wei Sun · Daisuke Yamashita · Sho Kanzaki · Tatsuo Matsunaga · Masato Fujii · Kimitaka Kaga · Kaoru Ogawa

Received: 10 July 2010 / Accepted: 6 January 2011 / Published online: 19 January 2011

Abstract Fibrocytes of the spiral limbus are thought to play a significant role in maintaining ion homeostasis in the cochlea. The present study measured physiological and morphological changes in spiral limbus of mice in response to noise exposure. 6-week-old male C3H/HeJJcl mice were exposed to octave-band noise (120 dB SPL) for 2 h and evaluated at a series of times thereafter, up to 8 weeks. Permanent hearing loss resulted in the mice, as assessed by auditory brainstem response (ABR) recordings. The fibrocytes loss was found in the spiral limbus of the apical turn, which has been proved to be induced by apoptosis. These results suggest that noise exposure might result in apoptosis of fibrocytes in spiral limbus, which suggest a mechanism for noise-induced hearing loss.

Keywords Spiral limbus · Fibrocytes · Noise · Hearing loss

Yong Cui and Guang-wei Sun equally contributed to this work.

Y. Cui · D. Yamashita · S. Kanzaki · K. Ogawa
Department of Otolaryngology,
School of Medicine, Keio University,
35 Shinanomachi, Shinjuku-ku,
Tokyo 160-8582, Japan

Y. Cui · G. Sun · D. Yamashita · T. Matsunaga · M. Fujii · K. Kaga
Laboratory of Auditory Disorders,
Division of Hearing and Balance Research,
National Institute of Sensory Organs,
National Tokyo Medical Center,
2-5-1 Higashigaoka, Meguro-ku,
Tokyo 152-8902, Japan

Y. Cui
Department of Otolaryngology,
Guangdong Academy of Medical Sciences
& Guangdong General Hospital,
106 Zhongshan Second Road,
Guangzhou 510080, People's Republic of China

G. Sun (✉)
Lab of Biomedical Material Engineering,
Dalian Institute of Chemical Physics,
The Chinese Academy of Sciences,
457 Zhongshan Rd, Dalian 116023, China
e-mail: sunrise124@gmail.com

Introduction

Histopathology associated with noise-induced hearing loss has been studied extensively and most of the research generally focused on pathological alterations in the hair cells and stereocilia [1–3]. The damage to other sensory structures, for example, afferent dendrites, and spiral ganglion cells (SGCs) can also lead to hearing loss [4, 5].

The functions of hair cells depend on the ionic homeostasis (especially K^+) in the endolymph, which is maintained by the K^+ recycling in the inner ear. The lateral wall and spiral limbus in the cochlea play an important role in the K^+ recycling, which can transport the K^+ ions actively by ion-exchange enzyme systems [6].

Hirose and colleagues [1, 7] characterized noise injury extending beyond the sensory structures to non-sensory structures (strial vascularis, spiral ligament and spiral limbus). In mice and other models, the morphological, enzymatic, and cytochemical features of the lateral wall, especially the stria, changed markedly hours and days after noise exposure [8–10].

Although the pathological change in the spiral limbus has been reported previously [1, 11–13], the time course of those morphological changes and the mechanism under them have not been well studied. In the present study, we tried to answer those questions.

Materials and methods

Animals and experimental groups

Male C3H/HeJJcl mice aged 6 weeks were used in the present study. Previous study showed that C3H mouse maintained excellent cochlear function throughout the first year of his age [14]. Animals were randomly assigned to serve as control or as noise-exposed subjects. The experimental groups included the following nine groups of mice ($n = 3$ per group) that were assessed 0, 6, 12, 24 h, 3 days, 1, 2, 4 and 8 weeks, respectively, after noise exposure. All mice underwent auditory brainstem response (ABR) threshold testing before being exposed to noise and immediately prior to killing. All experiments were conducted in accordance with the guidelines of the National Institutes of Health and the Declaration of Helsinki, and guidelines set by the Keio University Union on Laboratory Animal Medicine.

Noise exposure

Mice from each experimental group were placed in a custom-made sound chamber fixed within individual compartments of a metallic mesh cage which can hold four animals. The sound chamber was fitted with a speaker driven by a noise generator (AA-67N; RION Co., Ltd., Tokyo, Japan) and two power amplifiers (SRP-P150; Sony, Tokyo, Japan, and D-1405; Fostex, Chesterfield, MO). In all the experimental groups, the animals were exposed to one octave-band noise centered at 4 kHz, at 120 dB SPL for 2 h. Sound levels were calibrated and measured with a sound level meter (NL-20; RION Co., Ltd., Tokyo, Japan) placed at the level of the animal's head.

Auditory brainstem response (ABR) recordings

Auditory brainstem responses were evoked as described previously [15]. ABR recordings were performed with an extracellular amplifier Digital Bioamp system (BAL-1; Tucker-Davis Technologies, Alachua, FL), and waveform storing and stimulus control were performed with PowerLab systems Scope software (PowerLab 2/20; ADInstruments, Castle Hill, Australia). Sound stimuli were produced with a coupler type speaker (ES1spc; Bioresearch Center, Nagoya, Japan), which was inserted into the external auditory canal of each mouse. Mice were anesthetized with ketamine (80 mg/kg, i.p.) and xylazine (15 mg/kg, i.p.), and then implanted with stainless steel needle electrodes, which were placed at the vertex and ventrolateral to the left and right ears. Tone burst stimuli (0.1 ms rise/fall time; 1 ms flat segment) were used as test tones. Generally, the ABR waveforms were recorded for 12.8 ms at a sampling rate of 40,000 Hz using 50–5,000 Hz band-pass filter settings; waveforms from 1,024 stimuli at a frequency of 9 Hz were averaged. The ABR waveforms were recorded at 5 dB SPL intervals. The stimulus threshold was defined as the lowest sound level at which a recognizable waveform could still be seen. Because the sound level of test tones generated from the machine is limited, we set the stimulus threshold to 89.7, 91.7, and 83.2 dB SPL at 4, 8, and 16 kHz, respectively, when a mouse failed to respond due to profound noise-induced hearing impairment. The left and right ears of each mouse were used for ABR recording.

Histological preparations

After anesthetization with xylazine (15 mg/kg, i.p.) and ketamine (80 mg/kg), the animals were perfused transcardially with cold 0.01 M phosphate-buffered saline (PBS; pH 7.4), followed by 4% paraformaldehyde in 0.1 M PB. The left cochleas were extracted ($n = 3$, each time point), and a hole was made in the apex to allow intra-labyrinthine perfusion with the fixative. After overnight post-fixation in the same fixative at 4°C, cochleas were decalcified with buffered 0.1 M ethylenediaminetetraacetate (EDTA, pH 7.5) for 1 week at 4°C. Cochleas were dehydrated through a graded ethanol series and xylene, embedded in paraffin, and then sectioned in the midmodiolar plane at 5.0 μm. Light microscope: the slides containing cochlea sections were stained with hematoxylin and eosin (H&E) (Sakura Finetek Japan, Tokyo, Japan) to view the structure. The specimens were viewed with a laboratory microscope (DM 2500; Leica, Houston, TX). In the present study, the cochlea was divided into four half turns (lower basal, upper basal, lower apical, and upper apical). The fibrocytes in the spiral limbus of the lower apical turn were counted.

The cell density calculation was performed as described previously [16]. The cell density of fibrocytes in the spiral limbus, lateral wall and SGCs within the lower apical turn was calculated after H&E staining ($n = 15$, each time point). Area measurement and cell count were performed using ImageJ, a java-based image analysis program developed at the US National Institutes of Health.

Apoptosis detection

The TUNEL assay was performed with an apoptosis in situ detection kit (Wako, Osaka, Japan) according to the manufacturer's instructions ($n = 3$, each group). Negative controls were subjected to proteinase K digestion but not terminal deoxynucleotidyl transferase (TdT) treatment. Distilled water was substituted for TdT reagent in the negative controls.

The detection of anti-single-stranded DNA (ssDNA) was done as follows: after deparaffinization, the sections were

blocked with 10% normal goat serum (Sigma–Aldrich, St. Louis, MO) diluted in 0.01 M PBS for 60 min at room temperature. Incubation with primary and secondary antibodies was carried out in PBS containing 1% normal goat serum overnight at 4°C or for 1 h at room temperature. For negative controls, the primary antibody was omitted. Nuclear staining was performed with 4′6-diamidino-2-phenylindole dihydrochoride (DAPI, 1:1000; Sigma–Aldrich). The working dilutions and sources of the antibodies used in this study were as follows: rabbit ssDNA (1:200; Dako, Kyoto, Japan), Alexa Fluor 488 goat anti-mouse IgG (1:500; Molecular Probes, Eugene, OR,).

All tissue sections for one experiment were incubated for exactly the same time in all steps, and all images were collected using the same settings; thus, the differences in the intensity of staining reflect differences in the amount of bound antibody.

Statistical analysis

All statistical analyses were performed using one-way analysis of variance. SPSS 14.0 (SPSS for Windows; SPSS Inc., Chicago, IL, USA) was used for comparisons between experimental groups and control groups. $P < 0.01$ was considered significant.

Results

ABR recordings

ABR thresholds were recorded from control and seven groups of mice. Before noise exposure, each animal showed normal cochlear function (Fig. 1). For the noise-exposed groups, ABRs were recorded 0 h, 24 h, 3 days, 1, 2, 4, and 8 weeks, respectively, after noise exposure. Immediately after acoustic trauma (0 h) in the noise-exposed animals, the average threshold shift was 61.67, 88.33, and 79.17 dB SPL at 4, 8, and 16 kHz. Twenty-four hours after acoustic trauma, the threshold shift partially recovered and remained at this level for 8 weeks (Fig. 1). The stable threshold shift at 8 weeks after noise exposure suggested that the hearing loss in this model represents a permanent threshold shift (PTS).

Tissue processing for histology

To investigate the mechanism underlying noise-induced hearing loss, we stained cochlea from the noise-exposed mice with H&E stain and examined the cochlea for histopathological changes.

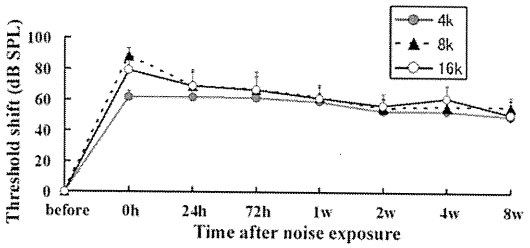

Fig. 1 Time course of threshold shifts following exposure to a one octave-band noise (centered at 4 kHz, 120 dB SPL) for 2 h. Threshold shifts were measured by recording auditory brainstem evoked responses (ABRs). ABR threshold increased immediately after noise exposure but recovered partially after 24 h and remained at this diminished level until the final ABR recording session (8 weeks after noise exposure), indicating that this type of acoustic trauma caused permanent hearing loss

Twelve hours after acoustic trauma, degenerating fibrocytes were present in spiral limbus within the apical turn of the cochlea; these cells displayed nuclear pyknosis and cytoplasmic vacuolation (Fig. 2f). Twenty-four hours after acoustic trauma, almost all fibrocytes in this region were gone (Fig. 2g). No recovery of fibrocytes was observed, even at 8 weeks (Fig. 2h).

By contrast, fibrocytes in the spiral limbus within the basal turn of the cochlea remained intact and displayed no apparent degenerative changes (Fig. 2b). Interdental cells in the spiral limbus were also unaffected by noise exposure; we did not observe degenerative changes during the entire observation period (Fig. 2).

In addition, under light microscopy, lateral wall, organ of Corti, SGCs appeared structurally well preserved at all time points following noise exposure (Fig. 2).

The number of fibrocytes in the spiral limbus and SGCs

Next, we quantified the cell number within the apical turn of the cochlea at seven time points after noise exposure, including the fibrocytes in the limbus, the SGCs, and the cells in lateral wall (Fig. 3). Since the upper apical turns in some preparations were destroyed as a result of the fixation procedure (a hole was made in the apex to facilitate fixation), we counted fibrocytes in the lower apical turn and SGCs. Five series of slides through mid-modiolus for each cochlea were used for cell counting ($n = 3$ cochleas).

For fibrocytes in the limbus, there was no significant fibrocytes loss 0 and 6 h after noise exposure. Twelve hours after exposure and thereafter, however, the number of fibrocytes in the spiral limbus decreased dramatically compared to that in the control group ($P < 0.01$) (Fig. 3a).

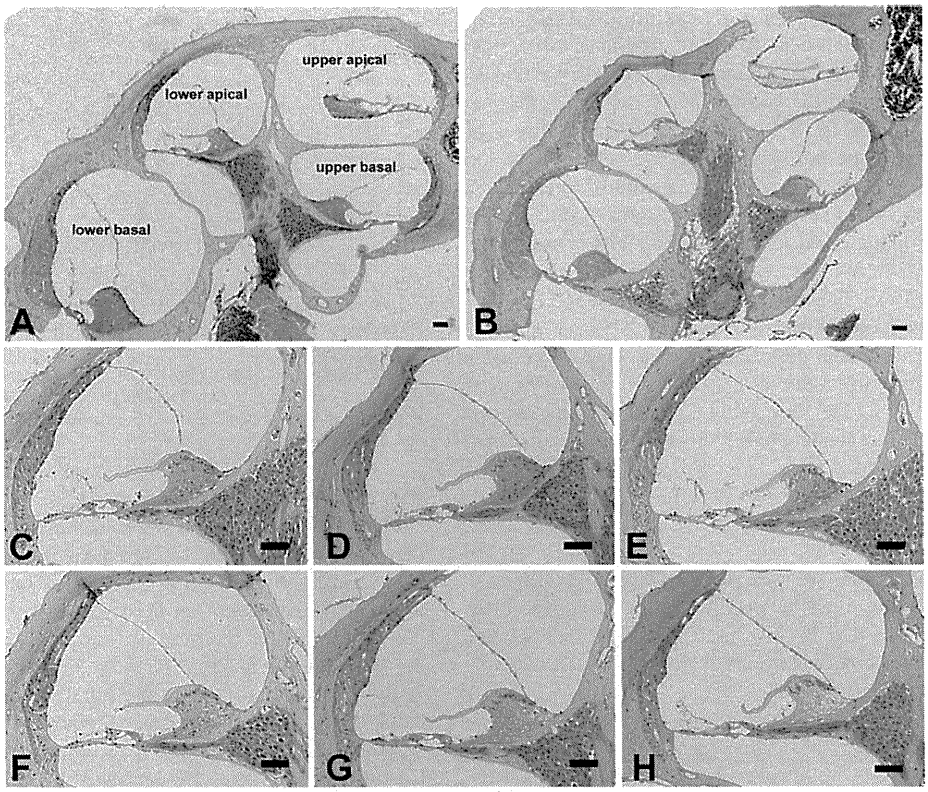

Fig. 2 H&E-staining within the lower apical turn of a mouse cochlea. **a**, **c** Control ear. **b**, **h** 8 weeks after nosie exposure. **d**, **e** Zero and six hours after exposure to 120 dB noise. No significant morphological changes were observed in the spiral limbus. However, 12 h after noise exposure, fibrocytes in the spiral limbus showed signs of degeneration and were noticeably fewer in number (**f**). Twenty-four hours after noise exposure, fibrocytes in the spiral limbus had disappeared completely (**g**). We observed no regeneration of fibrocytes in the spiral limbus 8 weeks after noise exposure (**h**). *Bar*: 25 μm

For SGCs (Fig. 3b) and spiral ligament (Fig. 3c), no significant cell loss was detected even at 8 weeks after noise exposure.

Apoptosis in the spiral limbus after noise exposure

To determine whether the noise-induced disappearance of fibrocytes in the spiral limbus was due to apoptosis, we analyzed cochleas from each group with ssDNA and TUNEL methods. Single-stranded DNA- and TUNEL-labeled cells were only found in the spiral limbus within the apical turns 12 h (Fig. 4c, g, j) and 24 h (Fig. 4d, h, k) after noise exposure. Thereafter, no apoptotic staining was present, even though fibrocyte loss was apparent.

No ssDNA- (data not shown) or TUNEL-labeled cells (Fig. 4) were found in the lateral wall, organ of corti, or spiral ganglion at any time prior to or after noise exposure.

Discussion

The loss of fibrocytes in the spiral limbus has been reported previously with sensory structure damage [1, 11–13]. Ohlemiller et al. noted that the loss of fibrocytes only happened in the apical turn just as our results. But no research paid attention to the time course and mechanism of the cell loss of fibrocytes in the spiral limbus. In our study, we found that the number of fibrocytes in spiral limbus within the apical turns of the cochlea began to decrease 12 h after noise exposure, a time ssDNA and TUNEL labeling was apparent in the fibrocytes of the spiral limbus. This means that the loss of fibrocytes in the spiral limbus within the apical turn was due to apoptosis. Since ssDNA and TUNEL are the common methods for detecting late-stage apoptosis, no TUNEL or ssDNA positive cells were detected until 12 h, initiation and progression of apoptosis

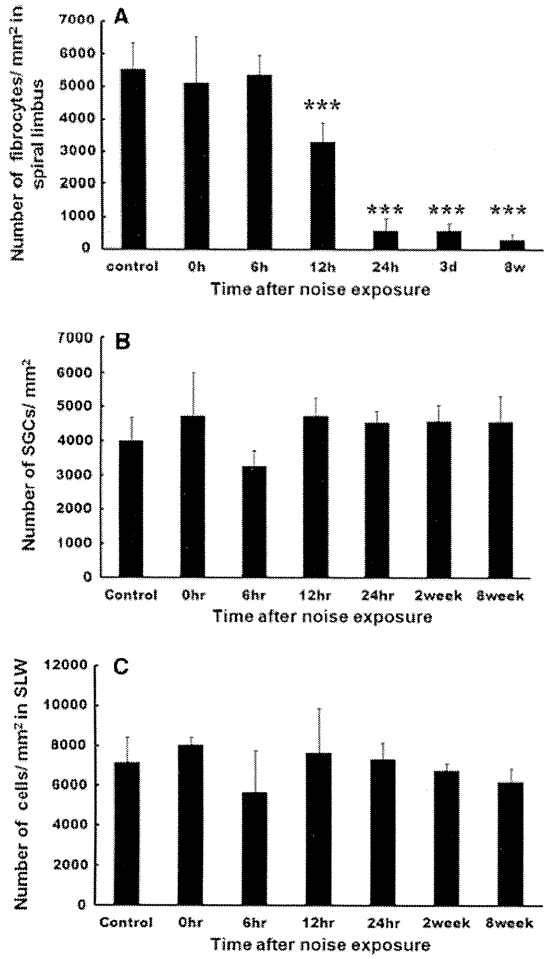

Fig. 3 The numbers of fibrocytes in the spiral limbus (a), SGCs (b) and cells in spiral ligament (c) within the lower apical turns of mouse cochlea. ***$P < 0.01$

of the fibrocytes in the spiral limbus may contribute to hearing loss at initial stage after noise exposure.

Noise exposure may lead to insufficiencies of cochlear blood flow [17], leading to ischemia and damage to capillary structure in the cochlea [18]. Ischemic damage leads to increased nitric oxide production, which causes cochlear cell damage [19]. Thus, noise-induced ischemia in cochlea might be associated with apoptosis in spiral limbus fibrocytes.

Ischemic damage, alteration in K^+ concentration, and acute energy failure induced by noise exposure may damage and cause dysfunction of fibrocytes in the spiral limbus. Twenty-four hours after noise exposure, a near complete loss of spiral limbus fibrocytes in the cochlea was detected only in the apical limbus, suggesting that noise-related injury to the limbus begins apically [11]. Interestingly, this may also occur in aging [20, 21], which is commonly associated with hearing loss.

Fibrocytes in the spiral limbus play a role in the inner route of the K^+ recycle in which the K^+ released from inner hair cells flows along the inner sulcus cells, fibrocytes and interdental cells back to the endolymph [6]. Loss of fibrocytes in the limbus induced by noise might disrupt K^+ recycling. Abnormal K concentration in the endolymph and the endocochlear potential (EP) has been reported to influence the activation of the hair cell, and then decrease the hearing level [7]. Minowa et al. [22] found that only the abnormality of the fibrocytes in the cochlea, with the normal appearance of the organ of Corti, the spiral ganglion even at the electron microscopy level, can lead to the sensorineural deafness in the mouse model of DFN3 nonsyndromic deafness. These results support our speculation that the fibrocytes play a critical role in the auditory function.

Several previous studies have shown that fibrocytes degenerate and ion transporter expression decreases in the spiral ligament after acoustic trauma [7, 23, 24]. In the present study, no significant changes have been found in

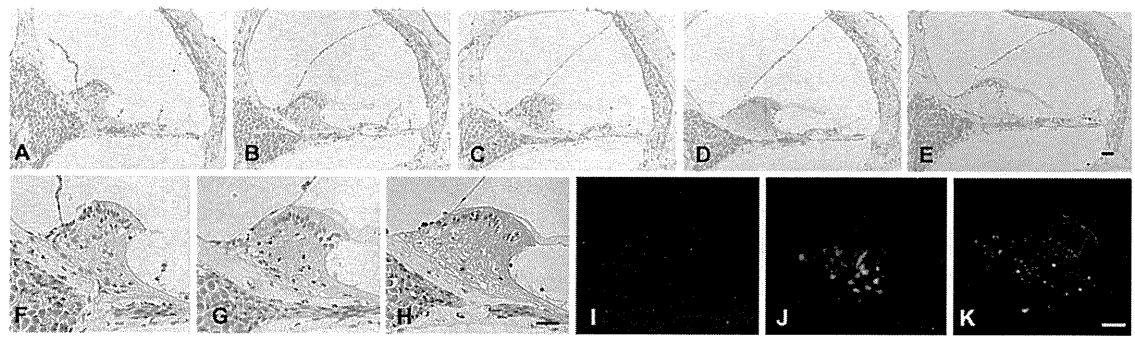

Fig. 4 TUNEL assay (**a–h**) and ssDNA staining (**i–k**) of the lower apical turn of the cochlea after noise exposure. **a**, **f**, **i** Control ear. **b** Six hours. **c**, **g**, **j** Twelve hours. **d**, **h**, **k** Twenty-four hours. **e** Eight weeks. *Bar*: 25 μm

the fibrocytes of spiral ligament. The genetic background of the mice which we used may account for this difference. The cochlear cells and structures in these mice may have different susceptibilities to noise-induced damage. Indeed, different strains of mice show marked variation in noise susceptibility [25, 26]. Ohlemiller [11] showed, for equal acoustic energy exposures, that CBA mice have a reduced EP and show cellular changes in lateral walls, while B6 mice have a normal EP and show little of the pathology seen in CBA mice.

Permanent changes in sensory structures after acoustic injury include hair cell loss, stereocilia damage, and neuronal loss [27], as well as loss of fibrocytes in the limbus and lateral wall, and strial degeneration [11]. In the present study, we did not observe damage in the organ of corti, spiral ganglion, and lateral wall. Several previous studies showed damage to the stereocilia only can lead to the hearing loss, including the PTS and temporary threshold shift (TTS) [27, 28]. Due to the type of histological material used in this study, we could not confirm whether stereocilia damage occurred or not. Although the loss of fibrocytes was only detected in the apical turn, a profound hearing loss was detected at 4, 8 and 16 kHz. Stereocilia damage might attributed to the wide hearing loss in this study.

Acknowledgments We thank Susumu Nakagawa and Han Liu for technical assistance. We also gratefully acknowledge the technical assistance provided by Masumi Furutani and Haruo Urata. This research was supported in part by a grant from the Society for Promotion of International Oto-Rhino-Laryngology (SPIO), Japan, to Y. Cui.

Conflict of interest We do not have any financial relationship with the organization that sponsored the research.

Reference:

1. Wang Y, Hirose K, Liberman MC (2002) Dynamics of noise-induced cellular injury and repair in the mouse cochlea. J Assoc Res Otolaryngol 3:248–268
2. Ou HC, Bohne BA, Harding GW (2000) Noise damage in the C57BL/CBA mouse cochlea. Hear Res 145:111–122
3. Nordmann AS, Bohne BA, Harding GW (2000) Histopathological differences between temporary and permanent threshold shift. Hear Res 139:13–30
4. Zhai SQ, Wang DJ, Wang JL, Han DY, Yang WY (2004) Basic fibroblast growth factor protects auditory neurons and hair cells from glutamate neurotoxicity and noise exposure. Acta Otolaryngol 124:124–129
5. Puel JL, Ruel J, Gervais d'Aldin C, Pujol R (1998) Excitotoxicity and repair of cochlear synapses after noise-trauma induced hearing loss. Neuroreport 9:2109–2114
6. Spicer SS, Schulte BA (1998) Evidence for a medial K^+ recycling pathway from inner hair cells. Hear Res 118:1–12
7. Hirose K, Liberman MC (2003) Lateral wall histopathology and endocochlear potential in the noise-damaged mouse cochlea. J Assoc Res Otolaryngol 4:339–352
8. Hsu CJ, Shau WY, Chen YS, Liu TC, Lin-Shiau SY (2000) Activities of Na(+), K(+)-ATPase and Ca(2+)-ATPase in cochlear lateral wall after acoustic trauma. Hear Res 142:203–211
9. Hsu CJ, Chen YS, Shau WY, Yeh TH, Lee SY, Lin-Shiau SY (2002) Impact of activities of Na(+)-K(+)-ATPase and Ca2(+)-ATPase in the cochlear lateral wall on recovery from noise-induced temporary threshold shift. Ann Otol Rhinol Laryngol 111:842–849
10. Hsu WC, Wang JD, Hsu CJ, Lee SY, Yeh TH (2004) Expression of connexin 26 in the lateral wall of the rat cochlea after acoustic trauma. Acta Otolaryngol 124:459–463
11. Ohlemiller KK, Gagnon PM (2007) Genetic dependence of cochlear cells and structures injured by noise. Hear Res 224:34–50
12. Kimura RS, Nye CL, Southard RE (1990) Normal and pathologic features of the limbus spiralis and its functional significance. Am J Otolaryngol 11:99–111
13. Liberman MC, Kiang NY (1978) Acoustic trauma in cats. Cochlear pathology and auditory-nerve activity. Acta Otolaryngol Suppl 358:1–63
14. Trune DR, Kempton JB, Mitchell C (1996) Auditory function in the C3H/HeJ and C3H/HeSnJ mouse strains. Hear Res 96:41–45
15. Masuda M, Nagashima R, Kanzaki S, Fujioka M, Ogita K, Ogawa K (2006) Nuclear factor-kappa B nuclear translocation in the cochlea of mice following acoustic overstimulation. Brain Res 1068:237–247
16. Komeda M, Roessler BJ, Raphael Y (1999) The influence of interleukin-1 receptor antagonist transgene on spiral ganglion neurons. Hear Res 131:1–10
17. Goldwin B, Khan MJ, Shivapuja B, Seidman MD, Quirk WS (1998) Sarthran preserves cochlear microcirculation and reduces temporary threshold shifts after noise exposure. Otolaryngol Head Neck Surg 118:576–583
18. Henderson D, Bielefeld EC, Harris KC, Hu BH (2006) The role of oxidative stress in noise-induced hearing loss. Ear Hear 27:1–19
19. Shi X, Nuttall AL (2003) Upregulated iNOS and oxidative damage to the cochlear stria vascularis due to noise stress. Brain Res 967:1–10
20. Ohlemiller KK, Gagnon PM (2004) Cellular correlates of progressive hearing loss in 129S6/SvEv mice. J Comp Neurol 469:377–390
21. Ohlemiller KK, Gagnon PM (2004) Apical-to-basal gradients in age-related cochlear degeneration and their relationship to "primary" loss of cochlear neurons. J Comp Neurol 479:103–116
22. Minowa O, Ikeda K, Sugitani Y et al (1999) Altered cochlear fibrocytes in a mouse model of DFN3 nonsyndromic deafness. Science 285(5432):1408–1411
23. Agrup C, Bagger-Sjoback D, Fryckstedt J (1999) Presence of plasma membrane-bound Ca(2+)-ATPase in the secretory epithelia of the inner ear. Acta Otolaryngol 119:437–445
24. Wangemann P (2002) K+ cycling and the endocochlear potential. Hear Res 165:1–9
25. Davis RR, Newlander JK, Ling X, Cortopassi GA, Krieg EF, Erway LC (2001) Genetic basis for susceptibility to noise-induced hearing loss in mice. Hear Res 155:82–90
26. Davis RR, Kozel P, Erway LC (2003) Genetic influences in individual susceptibility to noise: a review. Noise Health 5:19–28
27. Liberman MC (1987) Chronic ultrastructural changes in acoustic trauma: serial-section reconstruction of stereocilia and cuticular plates. Hear Res 26:65–88
28. Mulroy MJ, Curley FJ (1982) Stereociliary pathology and noise-induced threshold shift: a scanning electron microscopic study. Scan Electron Microsc 1753–1762

第3章 中耳真珠腫

松田 圭二
東野 哲也

キーワード

後天性真珠腫
一次性真珠腫
弛緩部型（上鼓室型）真珠腫
緊張部型真珠腫
再形成性真珠腫
遺残性真珠腫
乳突非削開型鼓室形成術
外耳道後壁削除型鼓室形成術
外耳道後壁保存型鼓室形成術
小児の癒着型真珠腫（緊張部型）

はじめに

中耳真珠腫は決して珍しい病気ではないが、単一施設に集積する症例数は比較的少ない。また進行性で多彩な病態を示す中耳疾患でもある。最も多い弛緩部型(上鼓室型)真珠腫を例にとると、聴力正常で陥凹部に少しdebrisが溜まる程度のものから、耳小骨連鎖が破壊され伝音難聴が高度なもの、さらに進んで外耳道後壁が大きく破壊されたり、迷路瘻孔、感音難聴、顔面神経麻痺、頭蓋内合併症などの重度合併症を示すものまで、進展に応じた多様な病態を示す。大部分の症例では耳漏の停止と聴力回復を目的に手術が行われる。しかし、再発することも稀ではなく難治性中耳炎の代表的な疾患とされる。

真珠腫の治療法を論じる際には、その対象となった症例の病態(重症度)が問題になる。大きく病態が異なるものでは、当然治療効果は変わるであろうし、施設間での比較、異なる手術法での成績比較などにも影響が大きい。手術症例の病型や進展度などに関して統一されたルールを共有する目的で、2008年に中耳真珠腫進展度分類案が日本耳科学会用語委員会から提出され[1]、2010年、同改訂案が出された[2]。これにより、術者間の症例把握が容易になり、さらに初学者の病態理解や術者養成教育にも効果が上がることが期待されている。今回は、この進展度分類に沿って後天性一次性真珠腫を中心に症例の解説を行いたい。

1 分類法

代表的な真珠腫分類法を表1に示す[3]。大きく先天性と後天性、さらに術後性を加えて3つに分類する。

先天性は、鼓室内真珠腫が鼓膜との連続性がないもので画像所見または鼓膜から透見できる白色病変として診断される。本邦では後上部にできることが多い。

後天性は一次性真珠腫(弛緩部型、緊張部型)と二次性真珠腫に分類される。一次性真珠腫のうち弛緩部型(上鼓室型)は最も高頻度に見られ弛緩部に陥凹ポケットが形成される。緊張部型では、後上部に陥凹ポケット・真珠腫が形成され、鼓膜の癒着が後上部に限局する後上部型(sinus cholesteatomaと同意)、緊張部全体が癒着した癒着型(tensa retraction cholesteatomaと同意)に分けられる。二次性真珠腫は、一見、慢性穿孔性中耳炎であるが穿孔縁から上皮が上鼓室方向に伸びたものである。

術後性真珠腫とは、真珠腫術後の再発を含め、医療行為の後に生じるものである。

小児と成人の真珠腫の違いについて

小児は、免疫機能が未熟で上気道感染の機会が多く中耳炎を合併しやすい。潜在的な先天性真珠腫の合併比率が高く、成人の一次性真珠腫とは異なる病態を示す。手術時には、発達した乳突蜂巣の隅々まで真珠腫が入り込む、真珠腫と肉芽組織との境界が不明瞭、あるいは鼓膜との連続性がない孤立性真珠腫が混在するなどの所見がしばしば見られ、遺残性再発を来しやすい。また、小児例では真珠腫の増大速度が早い例があることもよく知られており、副鼻腔炎をはじめとする上気道感染の併存は、耳管機能の未熟さとも相まって、再形成性再発を増やす要因となっている。一方、発達途中にある小児例では、耳管機能が年齢とともに改善されることが多い。いったん疾患のコントロールがつけば術後の再含気化も成人に比べより良く達成される。このような小児の特殊性を踏まえ、段階手術を選択することが一般的になりつつある。初回から後壁削除型術式をとるのは賢明ではないと考える術者も多い。また術後のフォローアップ間隔も成人より短く設定する必要がある。

【表1】中耳真珠腫の分類(文献3より引用改変)

1. 先天性真珠腫 (congenital cholesteatoma)

2. 後天性真珠腫 (acquired cholesteatoma)

1) 一次性真珠腫 (primary acquired cholesteatoma)
   ① 弛緩部型(上鼓室型)真珠腫
   (pars flaccida retraction cholesteatoma)
   ② 緊張部型真珠腫 (pars tensa retraction cholesteatoma)
   ・後上部型 (sinus cholesteatoma)
   ・癒着型 (tensa retraction cholesteatoma)

2) 二次性真珠腫 (secondary acquired cholesteatoma)

3. 術後性真珠腫 (post-operative cholesteatoma)

1) 再形成性真珠腫(狭義の再発) (recurrent cholesteatoma)

2) 遺残性真珠腫 (residual cholesteatoma)

3) 医原性真珠腫 (iatrogenic cholesteatoma)

4) 移植性真珠腫 (implantation cholesteatoma)

2 進展度分類

1 弛緩部型(上鼓室型)真珠腫

鼓膜弛緩部に陥凹ポケットが形成され、内部に白色のdebrisが溜まっていくタイプである。表2に日本耳科学会用語委員会提案の弛緩部型(上鼓室型)真珠腫の進展度分類2010改訂案を示す。図1にはそれぞれの進展度に相当する症例の鼓膜所見、模式図、CT所見を示す。進展度は術前の検査でおおむね予見可能であるが、最終的には術中所見で判断する。この分類法に基づき日本耳科学会用語委員4名の異なる施設における手術症例をレトロスペクティブに評価したものが図2である。各施設間でのばらつきはそれ程大きくないことが確認された。

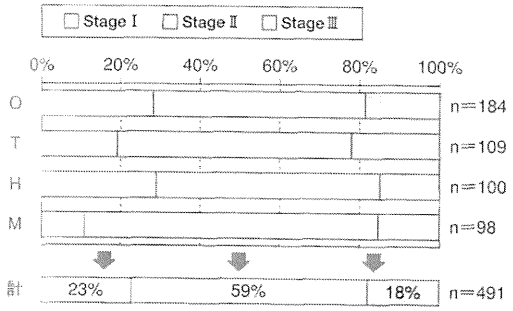

【図2】用語委員別の進展度分布(弛緩部型)。用語委員(O, T, H, M)別の弛緩部型(上鼓室型)真珠腫の進展度の分布を示す。平均はStage Ⅰが23%、Stage Ⅱが59%、Stage Ⅲが18%になった。文献1より引用

【表2】弛緩部型(上鼓室型)真珠腫進展度分類2010改訂案(基本分類)[2]

弛緩部型真珠腫: pars flaccida retraction cholesteatoma
(上鼓室型真珠腫: attic cholesteatoma)

弛緩部の陥凹から生じる真珠腫

Stage Ⅰ
真珠腫が上鼓室に限局
陥凹部の性状により2つの状態が区別できる
a:保存的治療で陥凹内の自浄能が保たれる状態
(いわゆる上鼓室陥凹)
b:陥凹内に貯留したdebrisの清掃が困難な状態
(記載例:弛緩部型真珠腫 Stage Ⅰb など)

Stage Ⅱ
真珠腫が上鼓室*を超えて乳突部や鼓室内に進展
*後方境界:キヌタ骨短脚後端またはfossa incudis
*下方境界:サジ状突起・鼓膜張筋腱~顔面神経管
*前方境界:サジ状突起・鼓膜張筋腱~上鼓室前骨板

Stage Ⅲ
次のような合併症・随伴病態を伴う
・顔面神経麻痺:FP (facial palsy)
・頭蓋内合併症:IC (intracranial complication)
・迷路瘻孔*:LF (labyrinthine fistula)
大きく窪んだ瘻孔(母膜を内骨膜から容易に剥離できない状態)
・高度内耳障害:LD (labyrinthine disturbance)
500, 1000, 2000 Hzのうち2周波数以上の骨導閾値がスケールアウト
・外耳道後壁の広汎な破壊:CW (canal wall destruction)
骨破壊の骨部外耳道前壁長の1/2程度を目安とする
・鼓膜全面*の癒着病変:AO (adhesive otitis)
鼓膜緊張部3/4象限以上の器質的な癒着を伴うもの
・真珠腫の錐体部進展:PE (pyramidal extension)
(記載例:Stage Ⅲ LD, Stage Ⅲ LF/CW など)

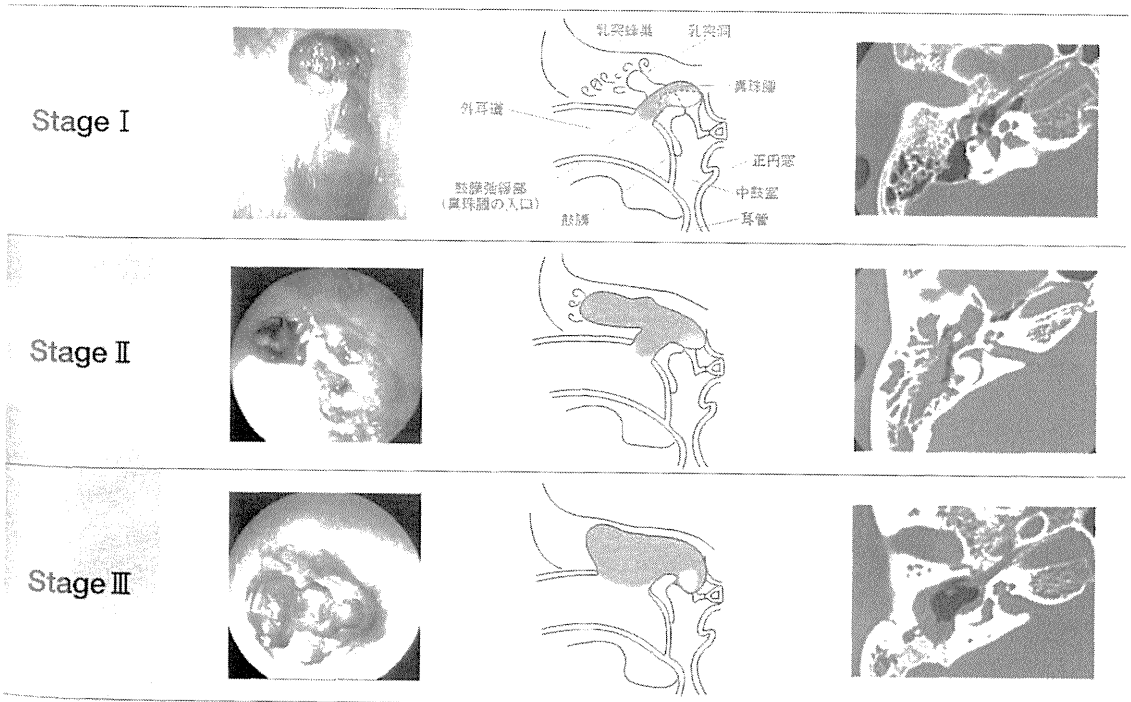

【図1】弛緩部型真珠腫の進展度別の鼓膜所見、模式図、CT所見(すべて右耳を示す)。Stage Ⅲには外耳道後壁の広汎な破壊例を示す。真珠腫の進展度にかかわらず、表2に示す合併症、随伴病態を伴う場合にはStage Ⅲに分類される

2 緊張部型真珠腫

鼓膜緊張部の後上部に陥凹ポケットが形成されdebrisが溜まっていくタイプで、後上部型（鼓室洞型，sinus cholesteatomaと同義）と癒着型（tensa retraction cholesteatomaと同義）の2型に分けられることもある。前者は、後上部から陥凹したポケットが鼓室洞を経て上鼓室、乳突洞方向に入っているが、鼓膜前半分には空気が入るなどして浮いているもの。癒着型は、後上部型と同じく後上部から陥凹ポケットが形成されるが、後上部型との違いは鼓膜緊張部全体（3/4象限以上）が岬角に癒着しているものを指す。表3に緊張部型真珠腫の進展度分類2010改訂案を示す。後上部型のうち真珠腫が後～下鼓室（鼓室洞）に限局しているものはStage Ⅰに、後上部型のうち真珠腫が鼓室洞から上鼓室や乳突洞に進展したものはStage Ⅱに、癒着型のすべてと後上部型のうち合併症があるものはStage Ⅲに分類される。図3に、それぞれの進展度に相当する症例の鼓膜所見、真珠腫進展模式図、CT所見を示した。

【表3】緊張部型真珠腫進展度分類2010改訂案（基本分類）[2]

緊張部型真珠腫：pars tensa retraction cholesteatoma

緊張部の陥凹から生じる真珠腫で、癒着型真珠腫、後上部型真珠腫、鼓室洞真珠腫などが含まれ、いわゆる二次性真珠腫や先天性真珠腫は除外する

Stage Ⅰ	真珠腫が後～下鼓室（鼓室洞）に限局 陥凹部の性状により2つの状態が区別できる a：保存的治療で陥凹内の自浄能が保たれ、癒着性中耳炎との区別が困難な状態 b：陥凹内に貯留したdebrisの清掃が困難 （記載例：Stage Ⅰbなど）
Stage Ⅱ	真珠腫が鼓室*を超えて上鼓室や前鼓室に進展 *上方境界：キヌタ骨短脚後端またはfossa incudis *前方境界：サジ状突起・鼓膜張筋腱～上鼓室前骨板
Stage Ⅲ	次のような合併症・随伴病態を伴う 合併症、随伴症状は、弛緩部型と同じ。鼓膜緊張部3/4象限以上の器質的な癒着（AO）を伴う「癒着型真珠腫」はここに分類される （記載例：Stage Ⅲ AO, Stage Ⅲ LD/CWなど）

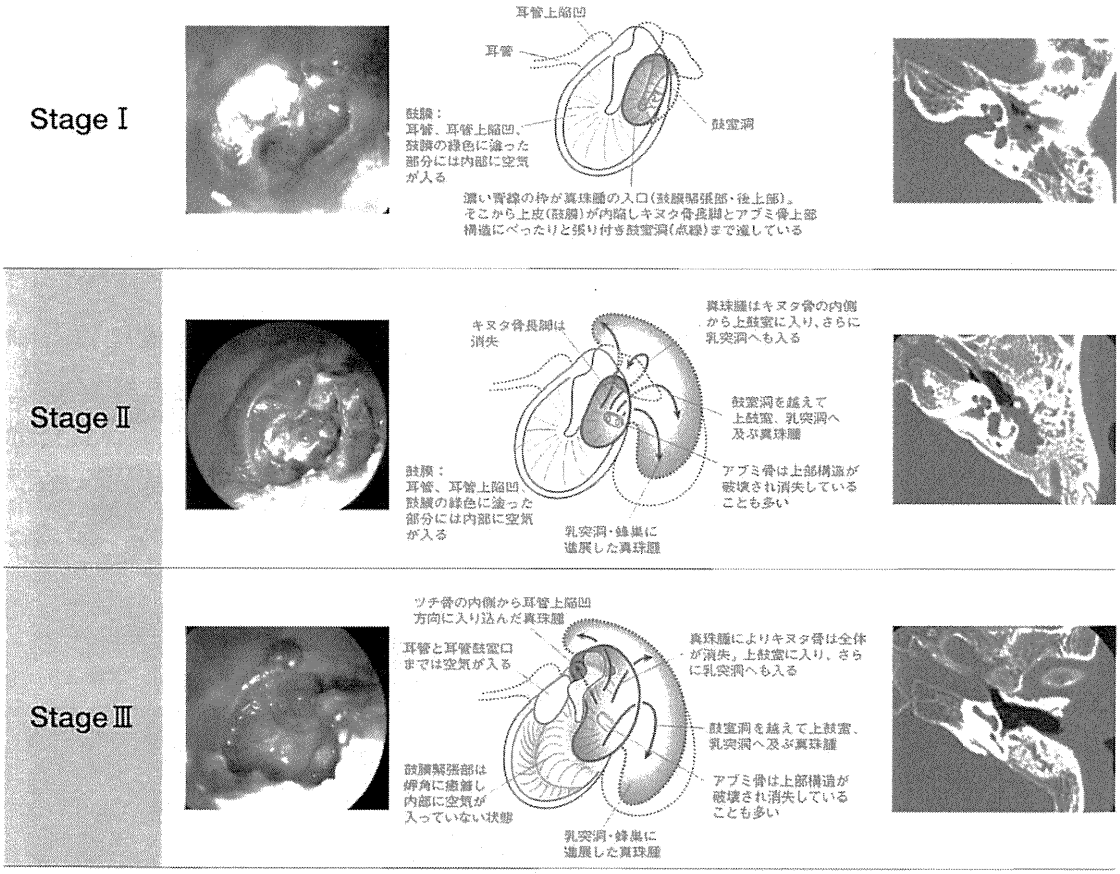

【図3】緊張部型真珠腫の進展度別の鼓膜所見、模式図、CT所見（すべて左耳を示す）。Stage Ⅰは、鼓室前半部分に含気腔を認め、鼓膜後上部の癒着鼓膜から鼓室洞に限局する真珠腫を形成したもの。Stage Ⅱは、Stage Ⅰと鼓膜所見は同じ後上部型であるが、真珠腫が鼓室洞を越えて上鼓室や乳突洞に達したもの。Stage Ⅲは、鼓膜緊張部全体の内陥・癒着に加え、鼓膜後上部がポケット状に深く内陥し上鼓室・乳突洞方向に真珠腫を形成した症例を示す（癒着型真珠腫と呼ばれる）。ただし進展度にかかわらず、表3に示す合併症、随伴病態を伴う場合にはStage Ⅲに分類される